Journal of Applied Fluid Mechanics, Vol. 8, No. 4, pp. 651-659, 2015.
Available online at www.jafmonline.net, ISSN 1735-3572, EISSN 1735-3645.
DOI: 10.18869/acadpub.jafm.67.223.19404

Upward Flow Boiling to DI-Water and Cuo Nanofluids Inside the Concentric Annuli

M. M. Sarafraz[1†], F.Hormozi[1], S. M. Peyghambarzadeh[2] and N. Vaeli[2]

[1]*Faculty of Chemical, Petroleum and Gas Engineering, Semnan University, Semnan, Iran*
[2] *Department of Chemical Engineering, College of Chemical Engineering, Mahshahr branch, Islamic Azad University, Mahshahr, Iran*

†*Corresponding Author Email: mohamadmohsensarafraz@gmail.com*

(Received December 14, 2012; Accepted September 18, 2014)

ABSTRACT

In this work, flow boiling heat transfer coefficients of deionized water and copper oxide water-based nanofluids at different operating conditions have been experimentally measured and compared. The liquid flowed in an annular space. According to the experiments, two distinguished heat transfer regions with two different mechanisms can be seen namely forced convective and nucleate boiling regions. Results demonstrated that with increasing the applied heat flux, flow boiling heat transfer coefficient increases for both of test fluids at both heat transfer regions. In addition to, by increasing the flow rate of fluid, the heat transfer coefficient dramatically increases at both regions. Influence of inlet temperature of fluid to the annulus as a complicated parameter has been investigated and briefly discussed. Results showed that inlet temperature of fluid displaces the boundary between forced convection and nucleate boiling areas such that with increasing the inlet temperature, nucleation mechanism become dominant mechanism at lower heat fluxes. Furthermore, higher heat transfer coefficient can be obtained due to interactions of bubbles and local agitations. Also, Chen type model was modified in terms of thermo-physical properties and examined to experimental data. Results showed that experimental data are in a good agreement with those of obtained by the correlation with deviation up to 30%.

Keywords: Flow boiling; Heat transfer; Pure distillated water; Forced convection; Annulus.

NOMENCLATURE

A	area, m^2
b	distance, m
Bo	Boiling number
C_p	heat capacity, $J.kg^{-1}.{}^oC^{-1}$
d_b	bubble departing diameter, m
d_h	hydraulic diameter, m
f	Fanning friction number
F	enhancement factor
h	enthalpy, $J.\ kg^{-1}$
ΔH_v	heat of vaporization, $J.kg^{-1}$
k	thermal conductivity, $W.m^{-1}.{}^oC^{-1}$
l_{th}	heated length, m
L	heater length, m
ΔL	characteristic length in Eq. (15), m
Nu	Nusselt number
Pe	Peclet number
Ph	Phase change number
Pr	reduced pressure
Pr	Prandtl number
P	pressure, Pa
q	heat, W
Re	Reynolds number
R_a	roughness, m
R_f	fouling resistance, m^2. K/ kW
s	distance, m
$\dot{X}$	Vapour mass fraction
X_{tt}	Martinelli parameter
y	vapor mass or mole fraction

Subscripts-Superscripts

b	*bulk*
bs	*base fluid*
nf	*nanofluid*
c	*critical*
fb	*flow boiling*
in	*inlet*
out	*outlet*
l	*liquid*
m	*mixture*
$\dot{m}$	*mass flux, kg/m^2.s*
n	*number of components*
nb	*nucleate boiling*
r	*reduced*
Sat	*saturated*
th	*thermometers*
v	*vapor*
w	Wall
α	*heat transfer coefficient, $W.m^{-2}.K^{-1}$*
ρ	*density, $kg.m^{-3}$*

S	suppression factor	κ	*Boltzmann constant = 1.381 ×10^{-23}, J. K^{1}*
T	temperature, K	φ	*volume fraction*
x	liquid mass or mole fraction	ϕ	*particle Sphericity*
μ	*viscosity, kg.m^{-1}.s^{-1}*		

1. INTRODUCTION

Flow boiling heat transfer of fluids has been studied extensively due to its wide application in industry. A large number of investigations for flow boiling inside horizontal and vertical tubes are available in the literature but only a few studies of saturated boiling were conducted in annular spaces. Early visualization experiments carried out by Hewitt et al. (1965) showed that the bubbles affect the nucleation activity. The presence of moving bubbles leads to the wave-induced nucleation phenomenon observed by Barbosa et al. (2003). It is noteworthy that boiling and two phase flow phenomena are used in a variety of industrial processes and applications, such as refrigeration, air-conditioning and heat pumping systems, energy conversion system, heat exchange systems, chemical thermal processes, cooling of high-power electronics components, cooling of nuclear reactors, micro-fabricated fluidic systems, thermal processes of aerospace station and bioengineering reactors (Lee et al., 2013). In the nuclear power applications, boiling heat transfer plays a key role both in the efficient energy transportation during the normal operation and in the successful decay heat removal for the transient accident condition, due to the large latent heat of water and the bubble-driven convection or turbulence. Specifically, to prevent the core melt down and to mitigate the leakage of radioactivity to the outside of reactor vessel, successful removal of decay heat is necessary (Cheng et al., 2013). Solid particles of the nominal size 1–100 nm are called nanoparticles, and low-concentration dispersions of such particles in a base fluid are called nanofluids. Nanofluids are known to apply a significant increase in thermal conductivity over that of the base fluid (Choi et al., 2003, Das et al., 2003, You et al. 2003, Ding et al. 2006). Early studies of application of nanofluids in flow and pool boiling have mainly focused on critical heat flux and surface characteristics of a heating section as well as thermal conductivity enhancement and the parameters that govern this behavior (Wen et al., 2005, Kim et al. 2006, Bang et al., 2006, Kim et al., 2007, Kim and Hu, 2007, Kim et al., 2009, Kim et al. 2010, Groeneveld, 1996, Joung et al., 2008, Joung et al., 2008). In fact, employing the nanofluids is a new research frontier related to nanotechnology and has found a wide range of potential applications particularly in cooling systems and two phase heat transfer applications. Following literature review represents the recent works conducted to forced convective and flow boiling heat transfer of nanofluids. An experimental study on the forced convective heat transfer and flow characteristics of TiO_2/water nanofluids under turbulent flow conditions has been reported by Duangthongsuk and Wongwises (Duangthongsuk-Wongwises, 2008). A horizontal double-tube counter flow heat exchanger is used in their study. They observed a slightly higher (6–11%) heat transfer coefficient for nanofluid compared to pure water. The heat transfer coefficient increases with increasing mass flow rate of the hot water as well as nanofluid. Recently, Sarafraz et al. conducted experimental investigations on pool heat transfer of DI-water and alcohols around the horizontal cylinder (Sarafraz, 2013, Sarafraz et al. 2014, Sarafraz-Peyghambarzadeh, 2012, Sarafraz et al., 2013). Also, among very few studies on flow boiling of nanofluids, Kim (Kim et al., 2006) represented about 50% enhancement in flow boiling CHF for Al_2O_3/water nanofluids flowing through a vertical stainless steel tube. Very recently, Henderson and his co-workers (Henderson et al. 2010) studied refrigerant-based SiO_2 and CuO-nanofluids in flow boiling experiments in horizontal copper tube. They found that while the boiling heat transfer coefficient (BHTC) of SiO_2/R-134a nanofluid decreases up to 55% in comparison to pure R-134a, the BHTC increases more than 100% for CuO-laden nanofluid over base fluid. Nanofluids are nominated as magical coolant for heat transfer applications. Thus, in this work, using a two-step method, CuO nanoparticles were dispersed into the DI-water and thermal performance of nanofluids has been compared to DI-water (as a traditional coolant). Also, influence of different operating parameters on the heat transfer coefficient of nanofluids and DI-water has been experimentally investigated. Results of this work can drastically help the researchers for designing the high efficiency cooling systems. Also, a modified Chen type model is introduced which can estimate the heat transfer coefficient of nanofluids with average error up to 30%.

2. EXPERIMENTAL

2.1 Experimental Setup

Fig. 1 depicts a summary of experimental apparatus that has been employed in presented work. This device is included with a vertical cylindrical glass vessel with diameter of 55 mm and height of 400mm that containing a stainless steel cylinder that dimensionally is 20mm in diameter and height of 300mm at the center of the glass vessel. Furthermore for the vessel, an annulus space has been created which allows the fluids to go around the heating section. At the center of stainless steel cylinder, a 1300W bolt heater has been embedded in which supplies the needed heat for creating the boiling phenomenon. To measure the surface temperature, four K-type thermocouples have been installed around the circumference of the cylinder near the surface. The arithmetic average of four readings was used to determine the heating surface To measure the inlet and outlet temperature of fluid.

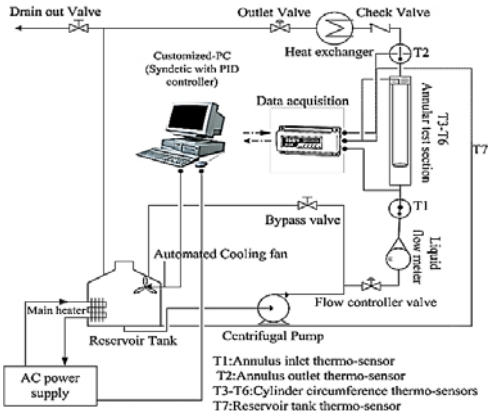

Fig. 1. Scheme of experimental apparatus.

into the annulus, two thermocouples have been used that arithmetic average of inlet and outlet temperature of annulus is considered as a bulk temperature of fluid flow inside the annulus. To calculate the real surface temperature by correcting the minor temperature drop due to the small distance between surface and thermocouple location, the Furrier's conduction equation is used as follows:

$$T_s - T_b = (T_{th} - T_b) - (s/k)(q/A) \quad (1)$$

In this equation, s is the distance between the thermocouple location and heat transfer surface and k is the thermal conductivity of the heater material. The value of s/k is determined for each thermocouple by calibration of the test heater. The average temperature difference was the arithmetic average of the four thermocouple locations. The boiling heat transfer coefficient, alpha, is calculated by following equation:

$$\alpha = \frac{\dot{m}.c.\left(T_{outlet} - T_{inlet}\right)}{\left(T_s - T_b\right)_{ave.}} \quad (2)$$

For each experiment, picture of boiling phenomena was taken using a ultra-high speed camera. Additionally, to remove the thermal contact resistant, silicone paste was injected into the thermocouple wells. The temperature of the liquid inside the tank is constantly monitored and controlled to any predetermined set point by a thermal regulator and PID controller. To prevent of temperature overshooting problem, due to the influence of released heat of bolt heater to the fluid, an air fan cooling has been installed at proper position near the reservoir tank. When the temperature of tank fluid turns higher than controller set point value, fan will start working to reduce the temperature of tank and turning back the temperature to the set point value. More details about the heating section are expressed in Fig. 2. To eliminate the influence of surface roughness on nucleate boiling and bubble generating, cylinder was polished several times using an emery paper with roughness 400. Also digital profile meter is employed to record the surface roughness of heating section which is given in Fig. 3. To record the generated bubbles, an ultra-high-speed camera has been employed which supports the edge cyber-shot technology for still images and videos up to frame rate 2000fps. Afterwards, the recorded images are overviewed and circumstances of bubbles can be studied.

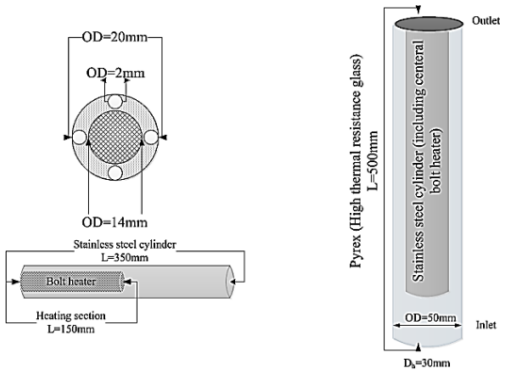

Fig. 2. Details and geometries of heating section.

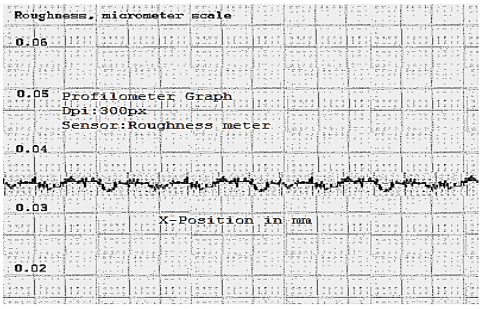

Fig. 3. Roughness of heating section.

To eliminate the influence of surface roughness on nucleate boiling and bubble generating, cylinder was polished several times using an emery paper with roughness 4 μm. Also digital profile meter is employed to record the surface roughness of heating section which is given in Fig. 3. As seen, roughness of surface is closely ranged from 0.03-0.04 μm that is considered as a standard smooth surface roughness.

The uncertainties of the experimental results are analyzed by the procedures proposed by Kline and McClintock (Kline-McClintock, 1953). The method is based on careful specifications of the uncertainties in the various primary experimental measurements. As seen from Eq. (2), the uncertainty in the measurement of the heat transfer coefficient can be related to the errors in the measurements of volume flow rate (v), hydraulic diameter (A), and all the temperatures as follows:

$$\alpha = f\ \{V, A_h, (T_{out} - T_{in}), (T_w - T_b)\} \quad (3)$$

$$\partial\alpha = \sqrt{\left[\left(\frac{\partial\alpha}{\partial V}\right)\delta V\right]^2 + \left[\left(\frac{\partial\alpha}{\partial A}\right)\delta A\right]^2 + \left[\left(\frac{\partial\alpha}{\partial(Tout-Tin)}\right)\delta(Tout-Tin)\right]^2 + \left[\left(\frac{\partial\alpha}{\partial(Tw-Tb)}\right)\delta(Tw-Tb)\right]^2} \quad (4)$$

According to the above uncertainty analysis, the uncertainty in the measurement of the heat transfer coefficient is 16.23%. Table 1 also represents the values of uncertainty relevant to experimentally used instruments. In this work, a large portion of errors are related to the temperature measurement and flow measurement. Since thermocouples are

not exactly mounted at surface, by employing the Wilson plot (Seara et al., 2007) real temperature of surface was estimated for each of thermocouple and reading temperatures were corrected accordingly.

Table 1 Uncertainties of instruments

Parameter	Instrument	Range	Uncertainty%
Voltage	Emersun autotrans	0-240 V	±0.1% readings
Current	Multi-meter Fluke Co.	0-8 A	±0.2% readings
Temperature	K-type thermocouple	0-700 ◦C	±0.3% readings
Flow rate	Flow meter Sarir-Teb Co.	10-600l/h	±0.1% readings

2.2 Preparation of Nanofluids

DI-water was selected as the main heat transfer fluid and copper composite nanoparticles, (NPs), (50nm, Purchased from Plasma Chem. GmbH, Germany) were uniformly dispersed into the base fluid for making a stable nanofluid (0.1 and 0. by wt. %). The two-step method was employed for preparation of nanofluid. Briefly, these processes include: Weight the mass of CuO NP with digital electronic balancer. The weighted NPs were added into the weighted DI-water while it was agitated in a clear flask. For better dispersing, the magnetic motorized stirrer was also employed to agitate the NPs suspension. UP400S ultrasonic Hielscher GmbH (400W / 24 kHz) was then used to remove the agglomeration and aggregations formed inside the bulk of nanofluids for about 4.5hr.

Quality tests were performed to control the morphology and size of nanoparticles as well as their purities. Fig. 4a shows the TEM image of CuO/water at wt. %=0.3. As can be seen, copper nanofluids have uniformly been dispersed into the base fluid and their size are in a good agreement with that of claimed by manufacturer.

Fig. 4b shows the result of XRD test which implies on this fact that there is no impurity other than copper oxide. Also, uniform peak shows the homogenous morphology of nanoparticles.

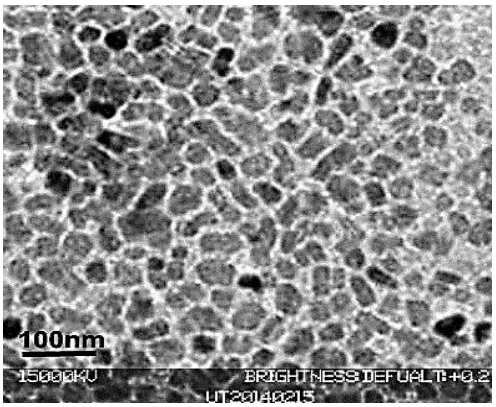

Fig. 4a. TEM image of CuO/water nanofluid.

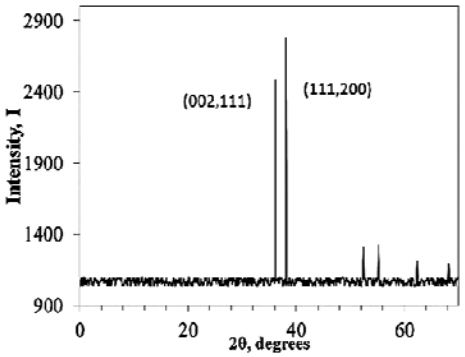

Fig. 4b. XRD pattern of CuO/water nanofluid.

3. RESULTS AND DISCUSSIONS

on this fact that there is no impurity other than copper oxide. Also, uniform peak shows the homogenous morphology of nanoparticles.There are many parameters which can influence on the thermal performance and heat transfer coefficient of fluid in a convective boiling flow. In this research, three important parameters are experimentally investigated and briefly discussed. Accordingly, heat flux, velocity of fluid (flow rate) and inlet sub-cooling temperatures are considered and influence of each of these parameters are separately investigated as follows.

3.1 Heat Flux

According to the experimental data, increase of flow boiling heat transfer coefficient is clearly observed in case of increasing the flow rate of fluid. This trend can be seen for DI-water and CuO/water nanofluid. In brief, increasing the heat flux directly increases the flow boiling heat transfer coefficient. However, from the particular heat flux, due to the bubble formation and presence the nucleate boiling phenomenon, higher flow boiling heat transfer coefficients are reported. As mentioned, the main reason of this fact refers to the bubble formation phenomenon and local agitations due to the interaction of bubbles including the coalescence and bubble collapsing around the heated surface. Fig. 5 typically represents the experimental data for flow boiling heat transfer coefficient of distillated water at various heat fluxes for inlet temperature of 343K.

As seen in Fig. 5, heat transfer coefficient of all coolants increases when rate of applied heat flux increases. This phenomenon was repeated for sub-cooling temperature of 353K and 363K. As can be seen in Fig. 5, from a particular heat flux (for instance, 46kW/m^2 at 343K for DI-water), slope of increase of heat transfer coefficient changes such that rate of increase of heat transfer coefficient significantly increases. This phenomenon is due to the changing the heat transfer mechanism from forced convective to nucleate boiling region. In this point, the first bubble may appear and local agitation would be formed. Also, at higher heat fluxes, bubble coalescence and bubble collapsing phenomenon lead the bulk of fluid to be locally agitated. Note that when a bubble collapses, micro-

tensions and micro-forces would be applied to the layers of fluid which subsequently generate the micro agitations around the heating section. This phenomenon drastically enhances the heat transfer coefficient and in this case, nucleate boiling heat transfer is the dominant mechanism. Note that with increasing the concentration of nanofluid, due to deposition of nanoparticles on the heating section, thermal resistance will be increased and heat transfer coefficient significantly deteriorates which can be seen in Fig. 5. More studies are needed for understanding the role of deposition on nucleate boiling of nanofluids which is currently undergone and is out of goals of this work.

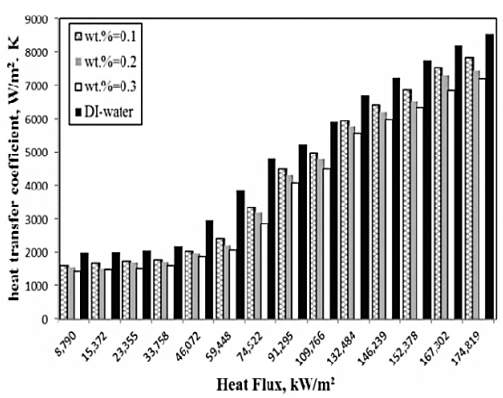

Fig. 5. Experimental flow boiling heat transfer coefficient of DI-water and copper nanofluids at 343K.

3.2 Fluid Flow Rate

As seen in Fig. 6, flow rate of fluid into the annulus, significantly, can influence on flow boiling heat transfer coefficient. In brief, by higher flow rate of fluid, higher heat transfer coefficient is recorded which means that there is a direct proportion between the velocity of fluid and flow boiling heat transfer coefficient which is clearly shown in Fig. 6:

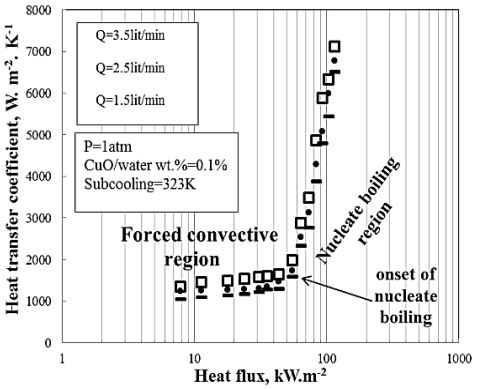

Fig. 6. Effect of different flow rate on flow boiling heat transfer coefficient of CuO/water nanofluids; similar behavior can be seen for DI-water.

3.3 Inlet Temperature

The significant influence of sub-cooling can only be seen on the Onset of Nucleate Boiling region (ONB). The ONB is considered as a boundary of separation of forced convective and nucleate boiling heat transfer regions, despite the first bubble may appear in this point. Briefly speaking, with increasing the sub-cooling temperature of fluid, heat flux corresponding with ONB point significantly decreases. However, a small increase of heat transfer coefficient at nucleate boiling region is reported, while, no significant influence on forced convective heat transfer coefficients can be seen. Fig. 6 represents the influence of sub-cooling temperature on the flow boiling heat transfer coefficient of CuO/water nanofluids. Fig. 8 comparatively demonstrates the influence of sub-cooling temperature on heat transfer coefficient of water and CuO/water nanofluid. As can be seen, a slight increase in heat transfer coefficient at nucleate boiling region is reported while no enhancement/deterioration of heat transfer coefficient in forced convective region can be seen.

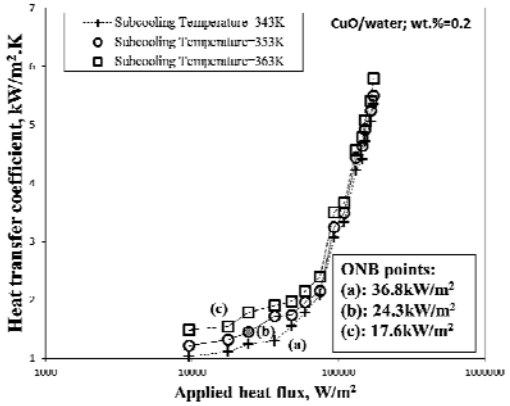

Fig. 7. Influence of sub-cooling temperature on heat transfer coefficient and ONB point of nanofluid.

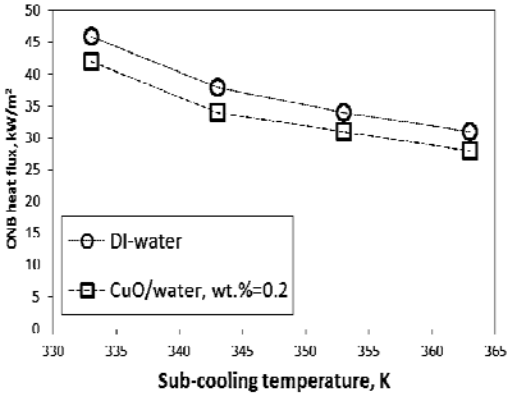

Fig. 8. Comparison between ONB heat flux in DI-water and CuO/water nanofluids.

As seen in Fig. 8, ONB heat fluxes deteriorate with increasing the inlet fluid temperature. In fact, the less, sub-cooling temperature, the lower ONB heat flux is reported for both of water and nanofluid. This trend leads the nucleate boiling region and forced convective regions to be changed based on the increase/decrease of ONB heat flux. For instance if forced convective mechanism is required, therefore, ONB heat flux should be

increased which means that lower inlet temperature (higher sub-cooling level) should be employed. On the other hand, as mentioned, ONB is a boundary point between forced convective and nucleate boiling region. In each of these areas, rate of heat transfer coefficient is totally different. Fig. 9 shows such trends in flow boiling heat transfer of DI-water. For nanofluids, similar behavior can be seen.

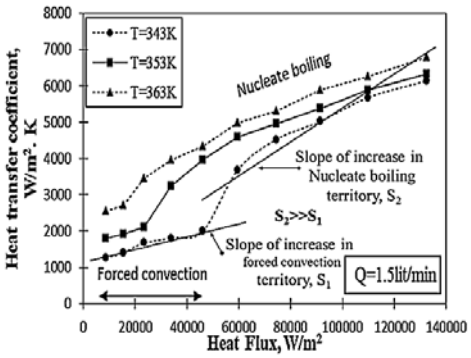

Fig. 9. Effect of different inlet temperature on the flow boiling and forced convective heat transfer of DI-water; different slopes represent different heat transfer mechanisms.

3.4 Visual Bubble Diameter

An overview of recorded images and video depicts that bubble formation phenomenon is a function of heat flux, flow rate (velocity of fluid) and inlet temperature of fluid. Although role and influence of heat flux in comparison with other factors is significant. According to the inferred results, at lower flow rate, larger bubbles are observed at any similar inlet temperature or heat fluxes. Likewise, results visually express that bubble diameter increases for higher heat fluxes at any similar inlet temperature and flow rate of fluid. But for the inlet temperature of fluid, there is no evident whether there is any influence on bubble diameter or not. In conclude the only effect of inlet temperature is on the ONB heat flux which helps investigators to determine the width of nucleate boiling and forced convection regions and dominant heat transfer mechanisms in cooling systems. Fig. 10 depicts the circumstances of bubble formation in flow boiling phenomenon for distillated water.As seen, at high heat fluxes (e.g. 132kW/m^2 in Fig. 9) bubble formation is tremendously complicated and detecting the bubbles discreetly is almost impossible but in lower heat fluxes, bubbles are clearly observed.

3.5 Correlating the Experimental Data

First step in correlating the experimental data is to estimate the thermo-physical properties properly. In this work, set of correlations were employed to estimate the physical properties of nanofluids. Note that for DI-water, thermo-physical properties are available in most well-known handbooks and literatures. Table 2 shows the correlations used for thermo-physical properties of nanofluids.

Properties of CuO nanoparticles have been given in Table 3 In this section, the HTC data for nanofluid are compared to those of obtained by Chen type model which is celebrated for its applicability to a broad range of pure, mixtures and refrigerants and

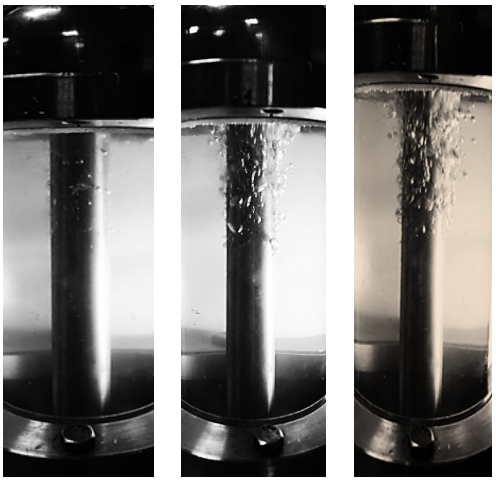

q=50kW/m^2 q=80kW/m^2 q=132kW/m^2

Fig. 10. Influence of increase of heat flux on bubble diameter and bubble generation.

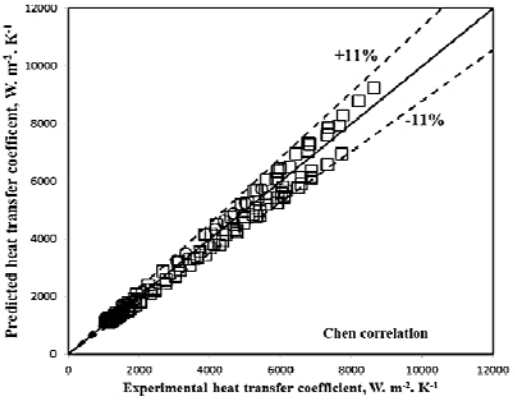

Fig. 11. Results of comparison between experimental data belonging to DI-water and those of obtained by correlation.

even nanofluids. The Chen correlation in its basic form is expressed as: Where α_{fc} is the convective heat transfer coefficient that may lonely be found for the liquid phase flowing. The parameter F is a multiplier that accounts for the apparent increase in velocity due to the presence of the vapor and is a function of the Martinelli parameter, X_{tt}. α_{nb} is the pool boiling heat transfer coefficient at the local wall superheat and can be calculated using any pure liquid pool boiling predicting correlations; The suppression factor, S, accounts

$$\alpha_{fb} = S.\alpha_{nb} + F.\alpha_{fc} \quad (5)$$

for the fact that α_{nb} is found from pool boiling correlations which over-predicts nucleate flow boiling. Coiller (Coiller et al., 1984) fitted the following equations to the graphical relationships for F and S:

$$F=\begin{cases} 1 & if\ \dfrac{1}{X_{tt}}\le 0.1 \\ 2.35\left(\dfrac{1}{X_{tt}}+0.213\right)^{0.736} & if\ \dfrac{1}{X_{tt}}\ge 0.1 \end{cases} \quad (6)$$

$$S=\frac{1}{1+2.53\times10^{-6}N_{\mathrm{Re}_{tp}}^{1.17}} \quad (7)$$

Table 2 Correlation used for estimating the thermo-physical properties of nanofluids

Physical properties	Correlation
Density	$\rho_{nf}=\varphi\rho_p+(1-\varphi)\rho_{bf}$
Heat capacity	$C_{pnf}=(1-\varphi)(\frac{\rho_{bf}}{\rho_{nf}})C_{pnf}+\varphi(\frac{\rho_p}{\rho_{nf}})C_{p_p}$
Viscosity	$\mu_{nf}=A(\frac{1}{T})-B$ $A=20587\varphi^2+15857\varphi+1078.3$, $B=-107.12\varphi^2+53.548\varphi+2.8715$
Thermal conductivity	$K_{nf}=\frac{K_p+(n-1)K_{bf}-\varphi(n-1)(K_{bf}-K_p)}{K_p+(n-1)K_{bf}+\varphi(K_{bf}-K_p)}K_{bf}+5\times10^4\beta\varphi\rho_{bf}C_{pbf}.\Pi$ $\Pi=\sqrt{\frac{\kappa T}{\rho_p d_p}}f(T,\varphi)$ $f(\varphi,T)=2.8217\times10^{-2}\varphi+3.917\times10^{-3}(\frac{T}{T_0})-3.0669\times10^{-2}\varphi-3.911\times10^{-3}$ $n=\frac{3}{\phi}$, ϕ : *Sphericity of nanoparticles*

Table 3 Properties Of Cuo nanoparticles

Nanoparticle	CuO
Average size, (nm)	45- 50nm
Purity	+99%
Thermal conductivity, (W/m. K)	74
Density, (g/cm^3)	7.03
Color	pale black
Surface area (m^2/g)	22.4

Other parameters can be estimated as follows:

$$X_{tt}=\left(\frac{1-\dot{x}}{\dot{x}}\right)^{0.9}\left(\frac{\rho_{bf}}{\rho_{nf}}\right)^{0.5}\left(\frac{\mu_{nf}}{\mu_v}\right)^{0.1} \quad (8)$$

$$N_{\mathrm{Re}_{tp}}=\frac{\dot{m}(1-\dot{x})d_h}{\mu_{nf}}F^{1.25} \quad (9)$$

Where:

$$\dot{x}=N_{ph}-N_{ph\,n}\exp\left(\frac{N_{ph}}{N_{ph_n}}-1\right) \quad (10)$$

$$N_{ph}=\frac{h_v-h_{l,sat}}{h_{fg}} \quad (11)$$

and:

$$N_{ph_n}=\frac{-N_{Bo}}{\sqrt{\left(\dfrac{455}{N_{pe_l}}\right)^2+0.0065^2}} \quad (12)$$

where:

$$N_{pe}=\frac{\dot{m}C_{p,nf}\,d_h}{\lambda} \quad (13)$$

$$N_{Bo}=\frac{\dot{q}}{\dot{m}.h_{fg}} \quad (14)$$

In this work, we added the correlations introduced in Table 2 into the Chen model and used the Gnielinski and Gorenflo for forced convective and nucleate boiling areas respectively. More information can be found in our previous study (Sarafraz-Hormozi, 2014). A rough comparison between calculated results and those of experimentally obtained shows that experimental data are in a fair/good agreements with calculated data with absolute average deviation of 30% and 11% for nanofluids and DI-water respectively. Figs 11-12 show the calculated results by proposed correlation in comparison with experimental data for nanofluids and DI-water respectively.

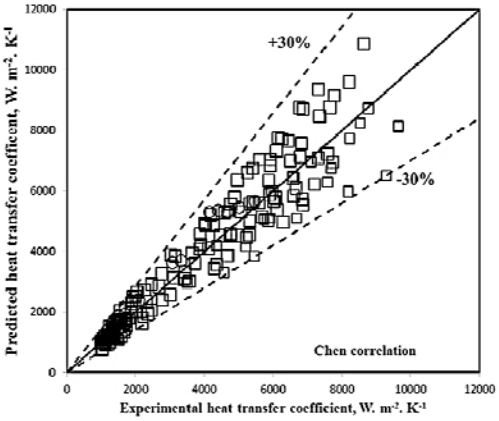

Fig. 12. Results of comparison between experimental data belonging to nanofluid and those of obtained by correlation.

Note that, to estimate the absolute average deviation of data following correlation was used:

$$AAD\% = \frac{1}{n}\sum_1^n\frac{\exp erimentaldata-calculated\ data}{\exp erimental\ data}\times100 \quad (15)$$

4. CONCLUSIONS

Experimental investigations on flow boiling heat transfer of distillated water and CuO nanofluids at different conditions inside a vertical annular space have been performed. Results demonstrated that heat transfer coefficient in flow boiling phenomenon is a function of various parameters such as heat flux, inlet temperature of fluid to annulus and velocity of fluids. Besides, bubble formation and condition of bubble formation were visually investigated. According to the results, heat transfer coefficient in flow boiling increases when applied heat fluxes increases. Noticeably, there are two heat transfer regions with different mechanisms and the boundary of these two regions is onset of nucleate boiling point, where the first bubble may appear. This region was a function of inlet temperature. Furthermore, inlet temperature assesses the width of each region and starting point of bubble formation phenomenon. Also, variations in flow rate of fluid showed that flow boiling heat transfer coefficient dramatically increases when velocity (flow rate) of fluid increases. In fact, flow rate of fluid is the most important factor of increase of the heat transfer coefficient in flow boiling phenomenon. However heat flux, similar to the flow rate has a significant influence on increasing heat transfer coefficient. In addition to, Recorded videos and images indicated that bubbles are larger when flow rate of fluid decreases and also are larger too when heat flux increases. But no influence is registered for effect of inlet temperature on bubble diameters.

ACKNOWLEDGEMENTS

The authors of this work dedicate this article to Imam Mahdi.

REFERENCES

Cheng, L. and L. Liu (2013). Boiling and two-phase flow phenomena of refrigerant-based nanofluids Fundamentals, applications and challenges. *Int. J. Refrigeration* 36, 421- 446

Chen, J. C. (1966). A correlation for boiling heat transfer to saturated fluids in convective flow, *Ind. Eng. Chem. Process Design Dev.* 5(3), 322-329.

Choi, S. U. S., Z. G. Zhang, W. Yu , F. E. Lockwood and E. A. Grulke (2001). Anomalous thermal conductivity enhancement in nanotube suspensions, *Appl. Phys. Lett.* 79 (14), 2252–2254.

Das, S. K., N. Putra and W. Roetzel (2003). Pool boiling characteristics of nanofluids, *Int. J. Heat Mass Trans*. 46(5), 851–862.

Ding, Y. H., D. AliasWen and R. A. Williams (2006). Heat transfer of aqueous suspensions of carbon nanotubes (CNT nanofluids), *Int. J. Heat Mass Trans.* 49(1–2), 240–250.

Duangthongsuk, W. and S. Wongwises (2008). effects of thermo-physical properties models on the predicting of the convective heat transfer coefficient for low concentration nanofluid, *Int. Comm. Heat Mass Trans.* 35, 1320-1326.

Groeneveld, C. (1996). the look-up table for critical heat fluxes in tubes, *Nucl. Eng.* 163, 1–23

Gungor, K. E. and H. S. Winterton (1986). a general correlation for flow boiling in tubes and annuli, *Int. J. Heat Mass Trans.* 29 (3), 351–358

He, Y., Y. Jin, H. Chen, Y. Ding, D. Cang and H. Lu (2007). Heat transfer and flow behavior of aqueous suspensions of TiO2 nanoparticles (nanofluids) flowing upward through a vertical pipe, *Int. J. Heat Mass Trans*. 50, 2272– 2281.

Henderson, K. , Y. G. Park, L. Liu and A. M. Jacobi (2010). Flow-boiling heat transfer of R-134a based nanofluids in a horizontal tube. *Int. J. Heat Mass Trans*. 5, 944–951.

Jeong, Y. H., M. S. Sarwar and S. H. Chang (2008). Flow boiling CHF enhancement with surfactant solutions under atmospheric pressure, *Int. J. Heat Mass Trans.* 51, 1913–1919.

Jeong, Y. H., W. J. Chang and S.H. Chang (2008). Wettability of heated surfaces under pool boiling using surfactant solutions and nanofluids, *Int. J. Heat Mass Tran.* 51, 3025–3031.

Kim, H., J. Kim and M. H. Kim (2006). Effect of nanoparticles on CHF enhancement in pool boiling of nanofluids, *Int. J. Heat Mass Trans*. 49(25–26), 5070–5074.

Kim, S. J. , I. C. Bang, J. Buongiorno and L. W. Hu (2006). Effects of nanoparticle deposition on surface wettability influencing boiling heat transfer in nanofluids, *Appl. Phys. Lett.* 89(15), 153-157.

Kim, H. D., J. B. Kim and M. H. Kim (2007). Experimental studies on CHF characteristics of nano-fluids at pool boiling, *Int. J. Multiphase Flow* 33, 691–706.

Kim, S. J., I. C. Bang, J. Buongiorno and L. W. Hu, (2007). Study of pool boiling and critical heat flux enhancement in nanofluids, *Bull Polish Academy Sci. Tech. Sci.* 55.

Kim, S. J., T. McKrell, J. Buongiorno and L. W. Hu (2009). Experimental study of flow critical heat flux in alumina–water, zinc-oxide–water and diamond–water nanofluids, *J. Heat Transfer* 131(4).

Kim, T. I. , Y. H. Jeong and S. H. Chang (2010). An experimental study on CHF enhancement in flow boiling using Al2O3 nano-fluid, *Int. J. Heat Mass Tran.* 53, 1015– 1022.

Kline. S. J. and F. A. McClintock (1953). Describing Uncertainties in Single-Sample Experiments, *Mechanical Engineering* 75, 3-8

Lee, T., J. H Lee and Y. H. Jeong, (2013). Flow boiling critical heat flux characteristics of magnetic nanofluid at atmospheric pressure and low mass flux conditions, *Int. J. Heat Mass Trans.* 56,101–106.

Peyghambarzadeh, S. M., S. H. Hashemabadi ,M. Naraki and Y. Vermahmoudi (2013). Experimental study of overall heat transfer coefficient in the application of dilute nanofluids in the car radiator, *Applied Therm. Eng.* 52, 8-16.

Sarafraz, M. M. (2013). Experimental Investigation on Pool Boiling Heat Transfer to Formic Acid, Propanol and 2-Butanol Pure Liquids under the atmospheric pressure, *J App. Fluid Mech.* 6(1), 73-79.

Sarafraz, M. M., S. M. Peyghambarzadeh, S. A. Alavi and N. Fazel Vaeli (2012). Nucleate pool boiling heat transfer of binary nano-mixtures under atmospheric pressure around a smooth horizontal cylinder, *periodica polytechnic, chem. Eng.* 56, 71–77.

Sarafraz, M. M., F. Hormozi and M. Kamalgharibi (2014). Sedimentation and convective boiling heat transfer of CuO-water/ethylene glycol nanofluids, *Heat mass trans. J.* 50, 1237-1249

Sarafraz, M. M. and S. M. Peyghambarzadeh (2013). Experimental study on sub-cooled flow boiling heat transfer to water–diethylene glycol mixtures as a coolant inside a vertical annulus, *Exp. Therm. Fluid Sci.* 50, 154-162.

Sarafraz, M. M and F. Hormozi (2014). Scale formation and sub-cooled flow boiling heat transfer of CuO–water nanofluid inside the vertical annulus, *Exp. Thermal Fluid Sci.* 52, 205-214

Seara, J. F., F. J. Uhia and J. Sieres (2007). Laboratory practices with the Wilson plot method, *Exp. Heat Trans.* 20, 123-135.

You, S. M. , J. H. Kim and K. H. Kim (2003). effect of nanoparticles on critical heat flux of water in pool boiling heat transfer, *Appl. Phys. Let.* 83(16), 3374–3376.

Wen, D. and Y. Ding (2005). Experimental investigation into the pool boiling heat transfer of aqueous based alumina nanofluids, *J. Nanopart. Res.* 7 (2), 2